Available online at www.sciencedirect.com

ScienceDirect

Ceramics International 40 (2014) 3793–3798

CERAMICS INTERNATIONAL

www.elsevier.com/locate/ceramint

Structural health monitoring capabilities in ceramic–carbon nanocomposites

Fawad Inam[a,*], Badekai R. Bhat[b,1], Thuc Vo[c,d,2], Walid M. Daoush[e,3]

[a]Northumbria University, Faculty of Engineering and Environment, Department of Mechanical and Construction Engineering, Newcastle upon Tyne, NE1 8ST, United Kingdom

[b]National Institute of Technology Karnataka, Department of Chemistry, Catalysis and Materials Laboratory, Surathkal, Srinivasanagar-575025, India

[c]Advanced Composite Training and Development Centre (Airbus), Hawarden CH5 3US, United Kingdom

[d]Glyndŵr University, Wrexham LL11 2AW, United Kingdom

[e]Helwan University, Faculty of Industrial Education, Department of Production Technology, Cairo, El Ameria Technology Complex, El Sawah Street, Egypt

Received 5 August 2013; received in revised form 10 September 2013; accepted 10 September 2013
Available online 16 September 2013

Abstract

A novel method for analysing structural health of alumina nanocomposites filled with graphene nanoplatelets (GNP), carbon nanotubes (CNTs) and carbon black nano-particles (CB) is presented. All nanocomposites were prepared using novel colloidal processing and then by Spark Plasma Sintering. Good homogeneous dispersion was observed for all carbon filled materials. Nanocomposite bars were indented to produce sub-surface damage. Change in electrical conductivities were analysed after indentation to understand structural damage. For correlating change in electrical conductivity and indentation damage and understanding damage tolerance, mechanical properties were compared. Because of the systematically induced indentation damage, a sharp decrease of 86% was observed in the electrical conductivity of CNT nanocomposite as compared to 69% and 27% in the electrical conductivities of GNP nanocomposites and CB nanocomposites respectively. CNTs impart superior damage sensing capability in alumina nanocomposites, in comparison to GNP and CB, due to their fibrous nature, high aspect ratio and high electrical conductivity.

Keywords: Carbon nanotubes; Graphene nanoplatelets; Carbon black; Alumina; Structural health monitoring

1. Introduction

Graphene and carbon nanotechnology [1] are becoming more and more ubiquitous because of the superlative combination of properties they offer to materials. They have been widely researched for their addition in polymer [2], ceramic [3–7] and metal [8] nanocomposites owing to the outstanding mechanical, thermal, and electronic properties attributed to them. Composite materials, filled with carbon nanofillers, are being researched for emerging applications like energy, transportation, defence, automotive, aerospace, sporting goods, and infrastructure sectors [9]. Particularly among ceramic based materials, CNTs have been reported to significantly improve mechanical, thermal and electrical properties of the ceramic nanocomposites [10]. For polymeric systems, carbon nanofillers have also proved to be very attractive because they offer structural damage sensing ability and the subject has been widely investigated [11–17].

Structural health monitoring (SHM) is a type of a Non-destructive Evaluation (NDE) technique that essentially involves the strategic embedding of conductive filler into a structure to allow continuous and remote monitoring for damage, deformation and failure. SHM technology is applied increasingly for research and industrial purposes as a potential tool for quality assurance [18,19]. However, many of the developed and available NDE technologies are complex, expensive and require significant calibration with the passage of time. Nanostructured carbon embedded polymeric systems have proven to be more sensitive towards structural damage [11–17]. However, the concept of self-sensing structural

*Corresponding author. Tel.: +44 191 227 3741.
E-mail address: fawad.inam@northumbria.ac.uk (F. Inam).
[1]Tel.: +91 824 2474000x3204; fax: +91 824 2474033.
[2]Tel.: +44 1978293979.
[3]Tel.: +20 106 683 2181; fax: +2 2 256 7850.

0272-8842/$ - see front matter © 2013 Elsevier Ltd and Techna Group S.r.l. All rights reserved.
http://dx.doi.org/10.1016/j.ceramint.2013.09.039

materials involving different types of carbon nanofillers is yet to be explored for ceramic composites, which is the subject of this research.

Most of the previous researched methods incorporating carbon nanofillers were based on the sensing of damage of long-fibre or woven reinforced brittle polymers [11–17]. Classifying cement as ceramics, damage sensing has been achieved in various studies with the incorporation of short carbon whiskers [20–22]. For cement composites with conductive fillers, self-sensing is made attainable by the damage and/or strain on the volume electrical conductivity of damaged or strained material [20–28]. Damage or stain affects the bulk conductivity to decrease, as reported for damage in the elastic regime [29], plastic (inelastic) deformation region [30,31] and after complete fracture [30]. Other researchers used carbon nanotubes instead of carbon fibre in cement for strain sensing applications and reported electrical conductivities decreasing upon tension [23] and increasing upon compression [24–27]. Luo et al. prepared hybrid cement composites using carbon whiskers and carbon nanotubes and reported superior sensing than the use of carbon nanotube as the sole conductive admixture [28].

Electrical conductivity sensing methods for alumina–carbon nanocomposites, essentially putting a voltage across the damaged sample and monitoring the change in resistance, have not yet been investigated in any research. To the best of authors' knowledge, there is no damage sensing research for advanced crystalline (granular) or amorphous (glass) ceramics using different types of carbon nanofillers (graphene nanoplatelets, carbon nanotubes and carbon black). In this work, damage is introduced systematically by Vickers indentation and damage sensing capabilities of graphene nanoplatelets, carbon nanotube and carbon black filled alumina nanocomposites are comprehensively analysed.

2. Experimental

Single-wall/double wall CNTs (Elicarb SWNT by Thomas Swan, UK: average outer diameter ~5 nm; lengths of up to 1 μm) were dispersed in dimethylformamide, DMF using high power tip ultrasonication for 30 min and then hand-mixed with alumina nanopowder (Sigma-Aldrich, UK: gamma phase; particle size <50 nm; surface area 35–43 $m^2\,g^{-1}$; melting point 2040 °C; and density 3.97 $g\,cm^{-3}$) for 5 min. As previously reported by Inam et al. [32], DMF was found to be a much more effective dispersant than ethanol for making stable, homogeneous CNT and composite dispersions. The liquid mixture was rotation ball milled for 7 h. It was then dried at 60 °C for 12 h using a rotary drier containing milling media (3 mm alumina balls), followed by vacuum oven drying at 100 °C for 48 h. To avoid re-agglomeration of carbon nanofillers during lengthy drying, the alumina balls (milling media) was added during rotary drying and this approach has not been previously reported. The dried powder mixture was ground and sieved at 250 mesh and then placed again in the vacuum oven at 100 °C for another 48 h to thoroughly extract the solvent. Nanocomposite pellets (diameter 20 mm and thickness 3 mm) were prepared by Spark Plasma Sintering (SPS), which is an advanced rapid processing technique for sintering advanced ceramic systems [33,34]. LABOX 350 (Sinter Land Inc, Japan) furnace was used for SPS. A pressure of 95 MPa was applied concurrently with the heating (rate 325 °C min^{-1}) and released at the end of the sintering period, which was 3 min for all of the samples. Maximum sintering temperature for all nanocomposites was 1600 °C. GNP and CB nanocomposites were prepared in the same way as the alumina–CNT nanocomposites. GNP nanopowder (grade A0-2; specific surface area: ~100 $m\,g^{-2}$; purity: 99%; average flake thickness: 20–30 monolayers) and CB (grade 633100: average particle size <50 nm) were supplied by Graphene Laboratories (USA) and Sigma-Aldrich (UK) respectively.

All of the sintered samples were ground using SiC paper down to 4000 grit. The density of the ground samples was measured using Archimedes' water buoyancy method. All samples were then thoroughly dried in an oven for 24 h and then diamond polished using 1 μm paste. A bar (dimensions: $18 \times 3 \times 3$ mm) was cut from each sintered pellet using a precision and deformation-free cutting machine (Accutom-50). At least 5 bars were produced for each composition. The Vickers indentations were performed using a Zwick microhardness tester (500 g load with 10 s of indentation time). Five indents (equally spaced) were produced on each bar and the bulk electrical conductivity of nanocomposites was measured at room temperature after every indentation. Four-point method (Fig. 1) was employed by using a resistivity/Hall measurement system (Sony Tektronix 370 A). The connecting wires in the experimental setup (Fig. 1) were permanently bonded by using silver paste in order to avoid any contact resistance for this comparative analysis. Vickers microhardness was calculated by $1.854(F/D^2)$, where F and D^2 are applied force and area of indentation respectively. For this work, sharp diamond indenter was used. Indentation fracture toughness was calculated using Anstis equation [35]. After indentation, fractured (top and cross-sectional) surfaces were gold coated and observed in an ultra-high resolution analytical FE-SEM (Hitachi, SU-70).

3. Results and discussion

In order to efficiently exploit the full potential of carbon nanofillers to improve the sensing capability in ceramics, it is important to have good dispersion of CNT in the ceramic matrix. The extraordinary large specific surface area of CNTs is the main hurdle for homogeneous dispersion and

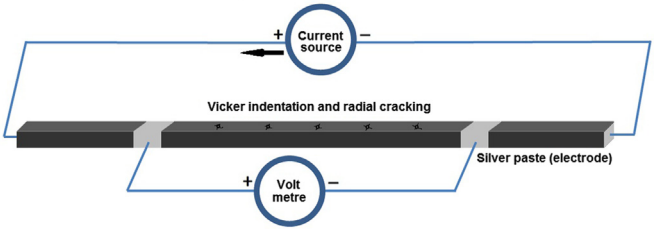

Fig. 1. Four-probe electrical conductivity measurement schematics of indented sample. Sample dimensions are $18 \times 3 \times 3$ mm.

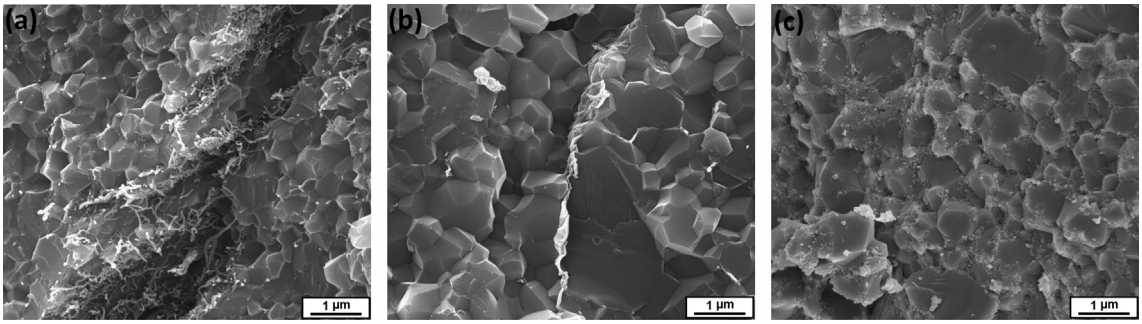

Fig. 2. Fractured surfaces showing: (a) alumina–2 wt% CNT nanocomposite; (b) alumina–2 wt% GNP nanocomposite; and (c) alumina–2 wt% CB nanocomposite.

de-bundling of CNTs. Though dispersion analysis is not the topic of this research, good dispersion was observed in all types of nanocomposites as evident in Fig. 2. Fig. 2a shows a fractured granular microstructure where a layer of CNT mesh (central fractured region) can be seen. Homogenously dispersed CNTs can also be observed in various isolated locations between alumina grains (Fig. 2a). Individual CB particles and GNP layer can be seen in Fig. 2b and c respectively. Therefore, it can be concluded that the combination of DMF dispersion and rotary drying in the presence of milling media, employed for the first time in this work, has proved to be an effective method for preparing homogeneously dispersed alumina–carbon nanocomposites.

Vickers indentation, at micrometre level, is currently used for ceramics to evaluate hardness and estimate fracture toughness. During Vickers indentation, ceramics fracture sub-surface (Hertzian cone crack) and from the tips of the diagonal indent to accommodate the penetrating diamond indenter [36]. Subsequently, new surfaces are created and radial-median and lateral crack systems are produced during loading and unloading of Vickers indenter (Fig. 3). For this work, Vickers indentation is used to compare the structural health monitoring in alumina nanocomposite because of its simplicity, non-destructive nature, and the fact that minimal machining is required to prepare the sample, as evident in this work. Following Vickers indentation, clear damage was visible to the unaided eye for all specimens. At the end of 5 Vickers indentations, all samples (alumina and nanocomposites) retained their integrity because of the small Vickers loadings after indentation. The load (500 g) was carefully selected to cause appropriate sub-surface damage for analysing electrical conductivities without completely fracturing the sample bars.

Electronic microscopy revealed radial cracking from the tip of the indent (Fig. 4a). The flaws detected as the result of indentation are very large compared to the critical flaw size that would control the strength of ceramics. The circled area was analysed for representative samples from each type of nanocomposite. CNTs were found to be in tension and couple of fractured and relaxed CNTs can also be seen (Fig. 4b). For alumina–2 wt% GNP nanocomposite, multi-layered graphene was also found to be bridging a radial crack upon indentation (Fig. 4c). This is consistent with the observations by Kvetkova et al. [7]. However, because of the wrinkles in multi-layered graphene (Fig. 4c), it appears to be in semi-relaxed state (non-tensed) which could be due to gold coating after the indentation. It should be noted that gold coating was done after 5 indentations to further enhance the image quality. For alumina–2 wt% CB nanocomposite, isolated CB particles were observed on the edges of the fractured surfaces (Fig. 4d). As compared to CNT and GNP nanocomposites, no crack bridging was observed for CB nanocomposites. This is due to their particulate nature.

Structural health monitoring for nanostructured carbon filled alumina composites was verified by measuring change in electrical resistivity after systematic introduction of damage to the samples. The experimental setup shown in Fig. 1 was specifically designed for the evaluation of the change in electrical conductivity during the systematically induced incremental damage. It should be noted that the connecting wires in the experimental setup (Fig. 1) were permanently bonded by using silver paste in order to avoid any contact resistance for this comparative analysis.

It is necessary to discuss the fracture, hardness and geometry of carbon nanofillers to understand the induced structural health monitoring capability. The change in the electrical conductivities of nanocomposite samples as a result of the deliberate damage (i.e. Vickers indentation) is shown in Fig. 5. Error bars represent good repeatability of measured values (Fig. 5). It is obvious from Fig. 5 that CNT and GNP filled nanocomposites were more sensitive towards the indentation damage as compared to CB filled nanocomposites (Fig. 5). After 5 indentations, the average electrical conductivity for CNT nanocomposites decreased from 84 to 12 S/m (i.e. a decrease of 86%). For GNP nanocomposites, a decrease of 69% was observed. For CB nanocomposites, the average electrical conductivity decreased from 11 to 8 S/m (i.e. a decrease of 27%). This is due to the fibrous nature of CNTs and layer-like features of GNP as opposed to particulate form of CB (Fig. 5). The origin of the damage sensing ability is attributed to the fracture of fibres that bridge microcracks and the consequent resistivity increase. The fracture of a bridging fibre occurs upon shear of a microcrack, with the resolved shear stress in the plane of the crack.

The different behaviour of the CNT and GNP modified matrix system and the carbon black modified matrix system has also to be attributed to the intrinsic structure of the percolated conductive paths in the composite. As reported in a review paper by Cho et al. [10] and observed in this work,

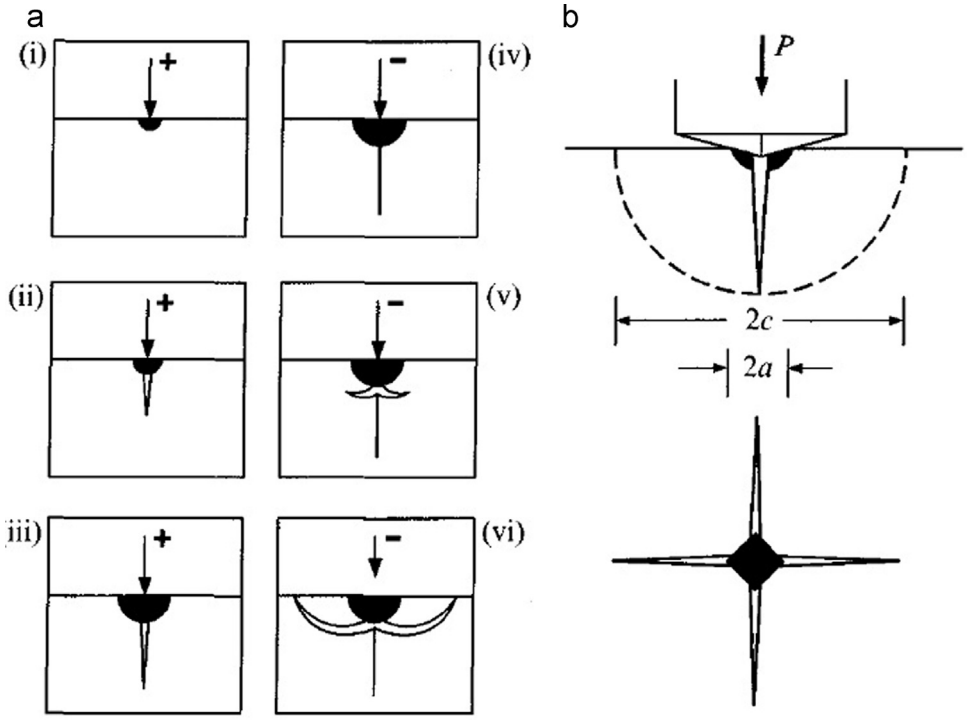

Fig. 3. Radial-median and lateral crack system: (a) evolution during complete loading (+) and unloading (−) cycle. Dark region denotes irreversible deformation zone; and (b) geometrical parameters of radial system [19].

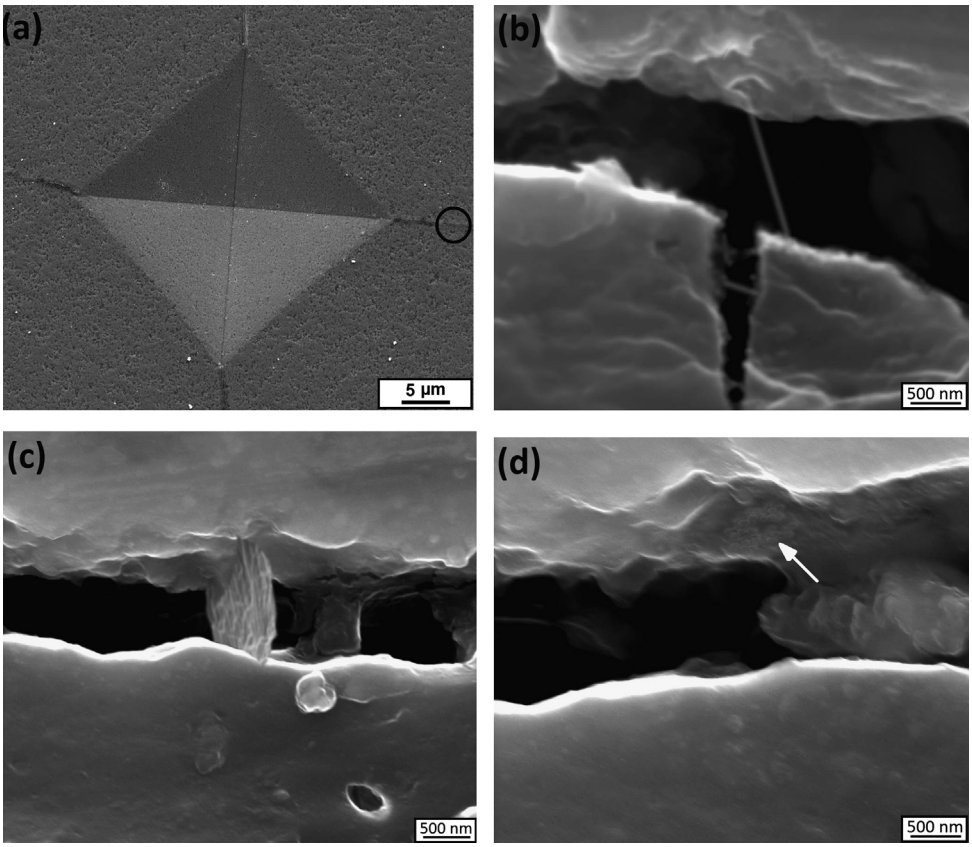

Fig. 4. Vickers indentation on alumina–2 wt% carbons nanocomposites showing: (a) indent and radial cracks; (b) crack bridging in CNT nanocomposite; (c) crack bridging in multilayered graphene nanocomposite; and (d) no crack bridging in CB nanocomposite. Arrow points CB agglomerates.

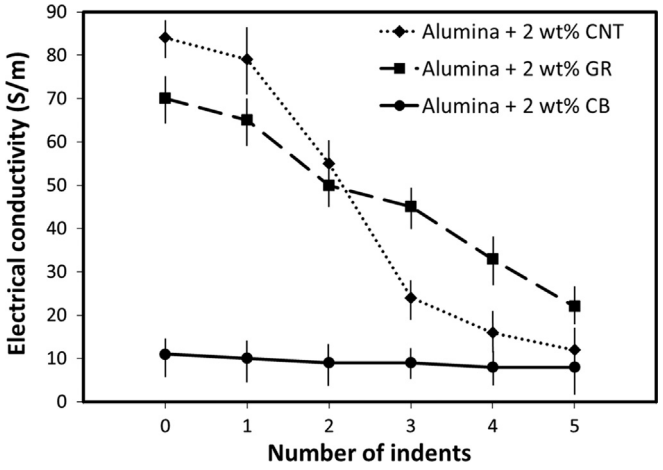

Fig. 5. Change in electrical conductivity due to Vickers indentation in alumina–carbon nanocomposites.

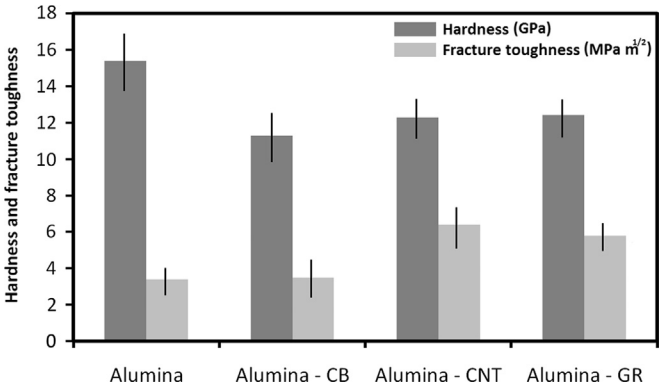

Fig. 6. Mechanical properties evaluated from Vickers indentation.

the electrical conductivity of CNT loaded systems tends to be approximately one to two orders of magnitude higher than that of carbon black composites, due to the higher intrinsic conductivity of CNTs and the much higher connectivity of the network. In this context, the high axial electrical conductivity of CNT and GNP not only offers the potential for fabricating conducting ceramics but also responsive ceramic systems. Also, it is obvious to understand that if CNTs and GNP are not homogeneously distributed and there is no separation (de-bundling) taking place among nano-fillers during the fracturing, such high sensitivity (Fig. 5) cannot be achieved.

For correlating change in electrical conductivity and indentation damage and understand damage tolerance, fracture toughness and hardness of samples were compared (Fig. 6). It was found that CNT and GNP nanocomposites have 14% and 10% higher fracture toughness, respectively, as compared to CB nanocomposites. This means that upon indentation, more damage was done by the penetrating diamond indenter for CB nanocomposites as compared to CNT and GNP nanocomposites. However, very small change in electrical conductivity was observed for CB nanocomposites. As reported [7,10], CNTs are responsible for improving fracture toughness of ceramics. As compared to CB nanocomposite, less damage was produced in CNT nanocomposites but a sharp decrease in electrical conductivity was observed. This elaborates that CNTs nanocomposite have superior damage sensing capability as compared to CB nanocomposites, which is due to the fibrous nature and high surface area of CNTs. It should be noted that the damage was solely caused by the indentation on the surface and sub-surface, which was responsible for inhibiting the electrical conductivity.

As compared to neat alumina, with a Vickers hardness of 15.4 GPa, decreases in hardness values were observed for CB, CNT and GNP nanocomposite samples (i.e. 11.3, 12.3 and 12.4 GPa respectively). This is primarily due to the lubricant nature of carbon nanofillers which is responsible for deeper penetration on the Vickers indenter during the indentation. These observations for the hardness of nanocomposites are in consistent with the studies conducted by different groups [3,7,37,38]. It is interesting to note that there is no significant difference in hardness for the different types of nanocomposites. However, because of the significant differences in the dimensions and geometry of carbonaceous fillers, their respective nanocomposites have very different damage sensing capabilities (i.e. irreversible change in electrical conductivities after damage).

4. Conclusion

Results in current work show that the change in electrical conductivity of the sample bars are highly dependent on the type of filler used and number of indentations or damage. Damage was indicated by an irreversible decrease in the electrical conductivity for the indented nanocomposite bars. Therefore, damage self-sensing by electrical conductivity measurement is an effective technique for carbon nanofiller reinforced alumina, as shown for Vickers indented specimens. These results demonstrate the high potential of carbon nanofillers (graphene nanoplatelets, carbon nanotubes and carbon black nano-particles) to be used for damage sensing in alumina nanocomposites. Carbon nanofillers were used to sense subsurface damage in alumina nanocomposites. As compared to CB, CNTs and GNP possess superior damage sensing ability in alumina nanocomposite structures due to their high aspect ratio (fibrous nature) and electrical conductivity. A sharp decrease of 86% and 69% were observed in the electrical conductivities of alumina–CNT and alumina–GNP nanocomposites, respectively, as compared to 27% in the electrical conductivity of alumina–CB nanocomposite due to indentation damage. Therefore, it is concluded that as compared to CB, CNT and GNP offer higher sensitivity for structural health monitoring to diagnose a structural safety and to prevent a catastrophic failure in brittle materials like alumina nanocomposites. This technique can also be used for damage sensing in glass matrices, which is subject of future research.

Acknowledgements

Dr. Fawad Inam would like to acknowledge generous support from Thomas Swan (UK) and Graphene Laboratories (USA) for supplying materials and their valuable time.

References

[1] S. Iijima, Helical microtubules of graphitic carbon, Nature 354 (1991) 56–58.

[2] F. Inam, T. Peijs, Transmission light microscopy of carbon nanotubes-epoxy nanocomposites involving different dispersion methods, Advanced Composites Letters 15 (2006) 7–13.

[3] A. Duszova, J. Dusza, K. Tomasek, G.S. Blugan, J. Kuebler, Microstructure and properties of carbon nanotube/zirconia composite, Journal of the European Ceramic Society 28 (2008) 1023–1027.

[4] K.K. Chew, K.L. Low, S.H. Sharif Zein, K.K. Chew, K.L. Low, S.H. Sharif Zein, D.S. McPhail, L.C. Gerhardt, J.A. Roether, A.R. Boccaccini, Reinforcement of calcium phosphate cement with multi-walled carbon nanotubes and bovine serum albumin for injectable bone substitute applications, Journal of the Mechanical Behavior of Biomedical Materials 4 (2011) 331–339.

[5] J. Cho, F. Inam, M. Reece, Z. Chlup, I. Dlouhy, M. Shaffer, A. Boccaccini, Carbon nanotubes: do they toughen brittle matrices?, Journal of Materials Science 46 (2011) 4770–4779

[6] Y. Fan, L. Wang, J. Lib, J. Lia, S. Sun, L. Chen, W. Chen, Jiang, Preparation and electrical properties of graphene nanosheet/Al_2O_3 composites, Carbon 48 (2010) 1743–1749.

[7] L. Kvetkova, A. Duszova, P. Hvizdos, J. Dusza, P. Kun, C. Balazsi, Fracture toughness and toughening mechanisms in graphene platelet reinforced Si_3N_4 composites, Scripta Materialia 66 (2012) 793–796.

[8] S.R. Bakshi, D. Lahiri, A. Agarwal, Carbon nanotubes reinforced metal matrix composites—a review, International Materials Reviews 55 (2010) 41–64.

[9] M.F.L. De Volder, S.H. Tawfick, R.H. Baughman, A.J. Hart, Carbon nanotubes: present and future commercial applications, Science 339 (2013) 535–539.

[10] J. Cho, A.R. Boccaccini, M.S.P. Shaffer, Ceramic matrix composites containing carbon nanotubes, Journal of Materials Science 44 (2009) 1934–1951.

[11] S.S. Lee, J.H. Lee, I.K. Park, S.J. Song, M.Y. Choi, Structural health monitoring for carbon fiber/carbon nanotube (CNT)/epoxy composite sensor, Key Engineering Materials 312–323 (2006) 290–293.

[12] L. Böger, M.H.G. Wichmann, L.O. Meyer, K. Schulte, Load and health monitoring in glass fibre reinforced composites with an electrically conductive, Composites Science and Technology 68 (2008) 1886–1894.

[13] N.D. Alexopoulos, C. Bartholome, P. Poulin, Z. Marioli-Riga, Structural health monitoring of glass fiber reinforced composites using embedded carbon nanotube (CNT) fibers, Composites Science and Technology 70 (2010) 260–271.

[14] S.V. Anand, D.R. Mahapatra, Quasi-static and dynamic strain sensing using carbon nanotube/epoxy nanocomposite thin films, Smart Materials and Structures 18 (2009) 045013.

[15] E.T. Thostenson, T.W. Chou, Carbon nanotube-based health monitoring of mechanically fastened composite joints, Composites Science and Technology 68 (2008) 1886–1894.

[16] A. Naghashpour, S.V. Hoa, In situ monitoring of through-thickness strain in glass fiber/epoxy composite laminates using carbon nanotube sensors, Composites Science and Technology 78 (2013) 41–47.

[17] V. Kostopoulos, A. Vavouliotis, P. Karapappas, P. Tsotra, A. Paipetis, Damage monitoring of carbon fiber reinforced laminates using resistance measurements. Improving sensitivity using carbon nanotube doped epoxy matrix system, Journal of Intelligent Material Systems and Structures 20 (2009) 1025–1034.

[18] D. Montalvão, N.M.M. Maia, A.M.R. Ribeiro, A review of vibration-based structural health monitoring with special emphasis on composite materials, The Shock and Vibration Digest 38 (2006) 295–324.

[19] C.C. Ciang, J.R. Lee, H.J. Bang, Structural health monitoring for a wind turbine system: a review of damage detection method, Nanotechnology 22 (2013) 045017.

[20] S. Wen, D.D.L. Chung, Electrical-resistance-based damage self-sensing in carbon fiber reinforced cement, Carbon 45 (4) (2007) 710–716.

[21] P. Chen, D.D.L. Chung, Carbon fiber reinforced concrete as an intrinsically smart concrete for damage assessment during static and dynamic loading, ACI Materials Journal 93 (4) (1996) 341–350.

[22] D.G. Meehan, S. Wang, D.D.L. Chung, Electrical-resistance-based sensing of impact damage in carbon fiber reinforced cement-based materials, Journal of Intelligent Material Systems and Structures 21 (1) (2010) 83–105.

[23] M. Saafi, Wireless and embedded carbon nanotube networks for damage detection in concrete structures, Nanotechnology 20 (2009) 395502.

[24] G.Y. Li, P.M. Wang, X. Zhao, Pressure-sensitive properties and microstructure of carbon nanotube reinforced cement composites, Cement and Concrete Composites 29 (2007) 377–382.

[25] X. Yu, E. Kwon, A carbon nanotube/cement composite with piezoresistive properties, Smart Materials and Structures 18 (2009) 055010.

[26] B. Han, X. Yu, E. Kwon, A self-sensing carbon nanotube/cement composite for traffic monitoring, Nanotechnology 20 (2009) 445501.

[27] B. Han, X. Yu, E. Kwon, J. Ou, Piezoresistive multi-walled carbon nanotubes filled cement-based composites, Sensor Letters 8 (2010) 344–348.

[28] J. Luo, Z. Duan, T. Zhao, Q. Li, Hybrid effect of carbon fiber on piezoresistivity of carbon nanotube cement-based composite, Advanced Materials Research 143–144 (2011) 639–643.

[29] J. Cao, S. Wen, D.D.L. Chung, Defect dynamics and damage of cement-based materials, studied by electrical resistance measurement, Journal of Materials Science 36 (18) (2001) 4351–4360.

[30] F. Reza, G.B. Batson, J.A. Yamamuro, J.S. Lee, Resistance changes during compression of carbon fiber cement composites, Journal of Materials in Civil Engineering 15 (5) (2003) 476–483.

[31] Y. Wu, C. Bing, W. Keru, Smart characteristics of cement-based materials containing carbon fibers, Master of Science in Mechanical Engineering (2003) 172–175.

[32] F. Inam, H. Yan, M. Reece, T. Peijs, Dimethylformamide: an effective dispersant for making ceramic–carbon nanotube composites, Nanotechnology 19 (19) (2008) 195710.

[33] B. Cui, D.D. Jayaseelan, W.E. Lee, Microstructural evolution during high-temperature oxidation of Ti_2AlC ceramics, Acta Materialia 59 (10) (2011) 4116–4125.

[34] H.F. Jackson, D.D. Jayaseelan, W.E. Lee, M.J. Reece, F. Inam, D. Manara, C.P. Casoni, et al., Laser melting of spark plasma-sintered zirconium carbide: thermophysical properties of a generation IV very high-temperature reactor material, International Journal of Applied Ceramic Technology 7 (3) (2009) 316–326.

[35] G.R. Anstis, P. Chantikul, B.R. Lawn, D.B. Marshall, Journal of the American Ceramic Society 64 (1981) 533–538.

[36] B. Lawn, Fracture of Brittle Solids, 2nd edition, Cambridge University Press, Cambridge, UK, 1993.

[37] Viktor Puchy, Pavol Hvizdos, Ján Dusza, Frantisek Kovac, Fawad Inam, Michael Reece, Wear resistance of Al_2O_3–CNT ceramic nanocomposites at room and high temperatures, Ceramics International 39 (5) (2013) 5821–5826.

[38] Fawad Inam, Andrew Heaton, Peter Brown, Ton Peijs, Michael Reece, Effects of dispersion surfactants on the properties of ceramic–carbon nanotube (CNT) nanocomposites, Ceramics International (2013), http://dx.doi.org/10.1016/j.ceramint.2013.06.031, in press.